Published in final edited form as:
Bioorg Med Chem Lett. 2009 May 1; 19(9): 2509–2513. doi:10.1016/j.bmcl.2009.03.030.

Inhibition of monoamine oxidase by (*E*)-styrylisatin analogues

Elizna M. Van der Walt[a], **Erika M. Milczek**[b], **Sarel F. Malan**[a], **Dale E. Edmondson**[b], **Neal Castagnoli Jr.**[c], **Jacobus J. Bergh**[a], and **Jacobus P. Petzer**[a,*]

a *Pharmaceutical Chemistry, School of Pharmacy, North-West University, Private Bag X6001, Potchefstroom, 2520, South Africa*

b *Departments of Biochemistry and Chemistry, Emory University, Atlanta, GA 30322, USA*

c *Department of Chemistry, Virginia Tech and Edward Via College of Osteopathic Medicine, Blacksburg, VA 24061, USA*

Abstract

Previous studies have shown that (*E*)-8-(3-chlorostyryl)caffeine (CSC) is a specific reversible inhibitor of human monoamine oxidase B (MAO-B) and does not bind to human MAO-A. Since the small molecule isatin is a natural reversible inhibitor of both MAO-B and MAO-A, (*E*)-5-styrylisatin and (*E*)-6-styrylisatin analogues were synthesized in an attempt to identify inhibitors with enhanced potencies and specificities for MAO-B. The (*E*)-styrylisatin analogues were found to exhibit higher binding affinities than isatin with the MAO preparations tested. The (*E*)-5-styrylisatin analogues bound more tightly than the (*E*)-6 analogue although the latter exhibits the highest MAO-B selectivity. Molecular docking studies with MAO-B indicate that the increased binding affinity exhibited by the (*E*)-styrylisatin analogues, in comparison to isatin, is best explained by the ability of the styrylisatins to bridge both the entrance cavity and the substrate cavity of the enzyme. Experimental support for this model is shown by the weaker binding of the analogues to the Ile199Ala mutant of human MAO-B. The lower selectivity of the (*E*)-styrylisatin analogues between MAO-A and MAO-B, in contrast to CSC, is best explained by the differing relative geometries of the aromatic rings for these two classes of inhibitors.

Keywords

Monoamine oxidase A; Monoamine oxidase B; Reversible inhibitor; Isatin; (*E*)-5-Styrylisatin; (*E*)-6-Styrylisatin

The oxidative deamination reaction catalyzed by monoamine oxidase B (MAO-B) is one of the major catabolic pathway of dopamine in the brain. Inhibitors of this enzyme lead to enhanced dopaminergic neurotransmission and are currently used in the symptomatic treatment of Parkinson's disease (PD).[1–4] Furthermore, MAO-B inhibitors also may exert a neuroprotective effect by reducing the concentrations of potentially hazardous by-products produced by MAO-B-catalyzed dopamine oxidation.[5] Considering that the human brain exhibits an age-related increase in MAO-B activity, inhibition of this enzyme is especially relevant in the treatment of PD.[6–8] The endogenous small molecule isatin (**1**) (Fig. 1) has been reported to be a moderately potent inhibitor of human MAO-B with an enzyme-inhibitor

*Corresponding author. Tel.: +27 18 2992206; fax: +27 18 2994243. E-mail adress: E-mail: jacques.petzer@nwu.ac.za (J.P. Petzer).

dissociation constant (K_i value) of 3 μM. Isatin also inhibits human MAO-A with a K_i value of 15 μM.[9] The three-dimensional structure of a complex between isatin and human recombinant MAO-B shows that isatin binds within the substrate cavity with the dioxoindolyl NH and the C-2 carbonyl oxygen hydrogen bonded to ordered water molecules in the active site (Fig. 2).[10] This binding mode leaves the entrance cavity of MAO-B unoccupied. The structure of isatin bound to MAO-A has not yet been determined.

Another small molecule, caffeine (**2**), is a weak inhibitor of MAO-B with a K_i value of 3.6 mM. The inhibition potency of caffeine is substantially increased by substitution at C-8 of the caffeinyl ring with a styryl side-chain. For example, (*E*)-8-(3-chlorostyryl)caffeine [CSC, (**3**)] (K_i = 0.086 μM) is approximately 45000 fold more potent as an inhibitor of baboon liver MAO-B than is caffeine.[11,12] Also of interest is the observation that CSC does not bind to MAO-A.[9] The improved inhibition potency and selectivity of CSC compared to caffeine has been explained by the possibility that (*E*)-styrylcaffeines span both the substrate and entrance cavities of MAO-B. This would allow for more productive van der Waals contacts with active site residues in both cavities that would lead to more potent inhibition.[11,13] In contrast, caffeine is expected to bind to either the substrate or entrance cavity, leaving the other cavity unoccupied. Human MAO-A has a single active site cavity whose geometry differs from that of MAO-B.[14] Data in the literature support the proposal that reversible inhibitors that span both cavities of MAO-B are more likely to exhibit selectivity for MAO-B over MAO-A. For example the crystal structures of relatively large reversible inhibitors, such as 1,4-diphenyl-2-butene,[10] farnesol[9] and safinamide[15] in complex with human MAO-B show that these inhibitors exhibit such a dual binding mode. In the present study we investigated the extent to which styryl substitution of isatin also may enhance isatin's MAO-B inhibition potency.

Inspection of the complex between isatin and human MAO-B[10] reveals that, in the substrate cavity, the dioxoindolyl ring is orientated with the 2-oxo group pointing towards the flavin cofactor while C-5 is directed in the general direction of the entrance cavity (Fig. 2). These structural features suggest that styryl substitution at C-5 would result in structures that traverse both cavities with the isatin moiety located in the substrate cavity with the C-5 styryl substituent extending into the entrance cavity. In contrast to the C-5 position, the C-6 position of isatin is directed towards the bottom of the substrate cavity. Extension of a C-6 styryl side chain into the entrance cavity would only be permitted if the isatin moiety adopted a different binding mode from that of isatin as observed in the human MAO-B crystal structure.[10]

To provide additional insights, molecular docking studies of (*E*)-5-styrylisatin (**4a**) and (*E*)-6-styrylisatin (**5**) (Scheme 1) in the active site of MAO-B were performed. For this purpose, the crystallographic structure of the complex of the reversible inhibitor safinamide and human recombinant MAO-B was selected (2V5Z.pdb).[15] This selection was based on the observation that the side chain of Ile-199, which acts as a "gate" that separates the entrance cavity from the substrate cavity,[10] is rotated out of its normal conformation to allow for the fusion of the two cavities and the accommodation of the larger structures. This fused cavity model of MAO-B allows for the possibility that **4a** and **5** may span both the entrance and substrate cavities. The docking calculations were performed using the LigandFit application of Discovery Studio 1.7 according to a previously reported protocol.[16,17] The top-ranked docking solution obtained for **4a** indicates that the styryl side chain extends beyond the boundary defined by the side chain of Ile-199 into the entrance cavity, while the dioxoindolyl ring is located in the substrate cavity (Fig. 2). The binding orientation of the dioxoindolyl ring of **4a** is similar to that of isatin with the 2-oxo and NH functional groups hydrogen bonded to water molecules present in the active site.[10] Structure **5** also spans both cavities with the styryl side chain located in the entrance cavity while the dioxoindolyl ring binds within the substrate cavity. In contrast to isatin and **4a**, the dioxoindolyl ring of **5** is rotated through ~180° to allow for access of the C-6 styryl side chain to the entrance cavity (Fig. 2). Based on these considerations, (*E*)-5-

styrylisatin (**4a**–**c**) and (*E*)-6-styrylisatin (**5**) analogues (Scheme 1) were synthesized and evaluated initially as inhibitors of baboon liver mitochondrial MAO-B and then as inhibitors of purified recombinant human MAO-B and MAO-A. Their respective inhibition potencies are compared to that of isatin.

Analogues **4a**–**c** of (*E*)-5-styrylisatin and (*E*)-6-styrylisatin (**5**) were synthesized in three steps (Scheme 1). Diethyl 4- or diethyl 3-nitrobenzylphosphonate (**6a**,**b**)[19] was condensed with the appropriate benzaldehyde (**7**) in the Wittig reaction to yield the 4- or 3-nitrostilbenes (**8a**,**b**), respectively.[20] Reduction of the nitrostilbenes with Sn/HCl led to the corresponding aminostilbenes (**9a**,**b**)[21] that, in turn, were treated with diethyl ketomalonate in the presence of acetic acid according to the literature description.[22] Following oxidative decarboxylation of the resulting 3-hydroxy-2-oxindolyl intermediate, the target (*E*)-styrylisatin analogues (**4**–**5**) were obtained.[22,23]

The MAO-B inhibitory properties of the (*E*)-styrylisatin analogues **4**–**5** initially were investigated using baboon liver mitochondrial fractions as a source of MAO-B and 1-methyl-4-(1-methylpyrrol-2-yl)-1,2,3,6-tetrahydropyridine (MMTP) as substrate.[12] These procedures have been documented in literature.[12] The baboon liver mitochondrial fractions were prepared according the procedure described in literature for the preparation of beef liver mitochondrial fractions.[24] In order to determine if the test compounds acted as time–dependent inactivators or reversible inhibitors of the enzyme, **4b** (40 nM) was preincubated with the mitochondrial fractions for periods of 0, 15, 30, and 60 minutes.[17] Since MAO-B activity remained unchanged, irrespective of the preincubation period (results not shown), it may be concluded that these (*E*)-styrylisatins interact reversibly with the active site of MAO-B. The inhibition potencies towards baboon liver mitochondrial MAO-B are presented in Table 1. All of the (*E*)-styrylisatin analogues were found to be more potent inhibitors of baboon liver MAO-B than isatin. For example, (*E*)-5-styrylisatin (**4a**) (IC_{50} = 41.7 nM) and (*E*)-6-styrylisatin (**5**) (IC_{50} = 444 nM) were approximately 200 and 19 fold more potent than isatin (IC_{50} = 8566 nM), respectively.

The MAO-B inhibitory properties of the (*E*)-styrylisatin analogues were also investigated using purified recombinant human MAO-B.[25] For all analogues tested, the modes of inhibition were found to be competitive (Fig. 3). As shown in Table 2 the (*E*)-styrylisatin analogues are 3 to 10-fold more potent than isatin as inhibitors of recombinant human MAO-B. These data provide evidence that potent MAO-B inhibitors result from structures that bind to both the entrance and substrate cavities. It was previously reported that the Ile-199 “gate” residue has significant functional importance in inhibitor binding and may be a determinant for the specificity of reversible MAO-B inhibitors.[9] The role of Ile-199 in the binding of **4**–**5** and of isatin to MAO-B was investigated using the human MAO-B I199A mutant protein. The results (Table 2) document that isatin and all of the (*E*)-styrylisatin analogues are slightly weaker inhibitors of the human MAO-B I199A mutant enzyme when compared to wild-type MAO-B. The Ile-199 residue therefore plays an important role in the binding interactions of these analogues. These data are consistent with the binding of (*E*)-styrylisatins in close proximity to Ile-199, a binding mode possible if the inhibitors traverse both active site cavities. Since the binding affinity of isatin to the I199A mutant protein is also reduced, hydration and/or structural alterations to the binding site cannot be ruled out and must await structural studies on this mutant form of MAO-B. According to the molecular docking studies, the functional groups of the inhibitors that may interact with Ile-199 are the styryl moieties of compounds **4**–**5**.

Interestingly, the (*E*)-styrylisatin analogues are also competitive inhibitors of recombinant human MAO-A,[26–28] with **4a** exhibiting the most potent inhibition (K_i = 0.78 μM). (*E*)-6-Styrylisatin (**5**) was the least potent inhibitor of MAO-A (K_i = 22 μM), and displayed the highest selectivity for MAO-B (39 fold) of all the isatin analogues tested. These results are surprising

since relatively large reversible inhibitors, such as 1,4-diphenyl-2-butene and CSC that occupy both the entrance and substrate cavities of MAO-B, exhibit selective inhibition of the MAO-B isoform and do not to bind to MAO-A.[9] To provide additional insights into this problem, molecular docking of **4a** and **5** in the active site of MAO-A were performed using LigandFit[16] as described before.[17] For this purpose, the crystallographic structure of the complex of human recombinant MAO-A with the reversible inhibitor harmine was selected (2Z5X.pdb).[14] As shown in figure 4, in the top-ranked docking solutions the dioxoindolyl rings of **4a** and **5** are positioned close to the FAD with the stryryl side chains extending towards the entrance of the active site cavity. These binding modes are similar to those observed with MAO-B. Also analogous to the docking results obtained with MAO-B is the dioxoindolyl ring of **5** which is rotated through ~180° compared to that of **4a**. Comparison of the structures of CSC with those of **4a** and **5** after energy minimization shows that CSC exhibits a planar structure where both rings occupy the same planar orientation (Fig. 5). In contrast, the styrylisatin analogues show the aromatic styryl ring is not coplanar with the isatin ring. For MAO-A inhibition by styrylisatins and styrylcaffeines a relatively larger degree of conformational freedom may be a requirement since the aromatic rings of **4a** and **5** (Fig. 4) adopt non-coplanar conformations in the MAO-A active site. Rigid coplanar styrylcaffeines such as CSC are therefore not expected to be MAO-A inhibitors.

In conclusion, (*E*)-5-styrylisatin and (*E*)-6-styrylisatin analogues have been identified as promising new probes of the binding sites of MAO-B and of MAO-A. The findings of this study support the hypothesis that the inhibition potencies of small molecule inhibitors of these flavoenzymes may be improved by substitution with side chains that promote binding to both the entrance and substrate cavities of MAO-B. The side chain of the Ile-199 “gate” in MAO-B appears to play an important role in the recognition of reversible inhibitors possibly by interacting with the styryl side chains of compounds **4**–**5** as well as other factors that will require additional structural information to identify. The surprising finding that (*E*)-styrylisatins are also competitive inhibitors of MAO-A, in contrast to results with CSC, shows that consideration of the relative geometries are factors important in the design of MAO inhibitors.

Acknowledgments

Financial support from the National Research Foundation and Medical Research Council, South Africa is acknowledged. This work was supported by National Institutes of Health grant GM-29433 (D.E.E.) and National Institute of Neurological Disorders and Stroke award number F31NS063648 (to E.M.M.). The content of this publication is solely the responsibility of the authors and does not necessarily represent the official views of the National Institute of Neurological Disorders and Stroke or the National Institutes of Health.

References and notes

1. Youdim MB, Collins GG, Sandler M, Bevan Jones AB, Pare CM, Nicholson WJ. Nature 1972;236:225. [PubMed: 4553640]
2. Collins GG, Sandler M, Williams ED, Youdim MB. Nature 1970;225:817. [PubMed: 5415111]
3. Di Monte DA, DeLanney LE, Irwin I, Royland JE, Chan P, Jakowec MW, Langston JW. Brain Res 1996;738:53. [PubMed: 8949927]
4. Finberg JP, Wang J, Bankiewich K, Harvey-White J, Kopin IJ, Goldstein DS. J Neural Transm Suppl 1998;52:279. [PubMed: 9564628]
5. Youdim MBH, Bakhle YS. Br J Pharmacol 2006;147:S287. [PubMed: 16402116]
6. Nicotra A, Pierucci F, Parvez H, Senatori O. Neurotoxicology 2004;25:155. [PubMed: 14697890]
7. Fowler JS, Volkow ND, Wang GJ, Logan J, Pappas N, Shea C, MacGregor R. Neurobiol Aging 1997;18:431. [PubMed: 9330975]
8. Karolewicz B, Klimek V, Zhu H, Szebeni K, Nail E, Stockmeier CA, Johnson L, Ordway GA. Brain Res 2005;1043:57. [PubMed: 15862518]

9. Hubálek F, Binda C, Khalil A, Li M, Mattevi A, Castagnoli N Jr, Edmondson DE. J Biol Chem 2005;280:15761. [PubMed: 15710600]
10. Binda C, Hubálek F, Restelli N, Edmondson DE, Mattevi A. Proc Natl Acad Sci U S A 2003;100:9750. [PubMed: 12913124]
11. Vlok N, Malan SF, Castagnoli N Jr, Bergh JJ, Petzer JP. Bioorg Med Chem 2006;14:3512. [PubMed: 16442801]
12. Pretorius JP, Malan SF, Castagnoli N Jr, Bergh JJ, Petzer JP. Bioorg Med Chem 2008;16:8676. [PubMed: 18723354]
13. Van den Berg D, Zoellner KR, Ogunrombi MO, Malan SF, Terre'Blanche G, Castagnoli N Jr, Bergh JJ, Petzer JP. Bioorg Med Chem 2007;15:3692. [PubMed: 17416530]
14. Son S-Y, Ma J, Kondou Y, Yoshimura M, Yamashita E, Tsukihara T. Proc Natl Acad Sci USA 2008;105:5739. [PubMed: 18391214]
15. Binda C, Wang J, Pisani L, Caccia C, Carotti A, Salvati P, Edmondson DE, Mattevi A. J Med Chem 2007;50:5848. [PubMed: 17915852]
16. Accelrys Discovery Studio 1.7, Accelrys Software Inc., San Diego, CA, USA. 2006, http://www.accelrys.com.
17. Ogunrombi MO, Malan SF, Terre'Blanche G, Castagnoli N Jr, Bergh JJ, Petzer JP. Bioorg Med Chem 2008;16:2463. [PubMed: 18065227]
18. Yasara Structure, Yasara Biosciences, Graz, Austria. 2008, http://www.yasara.org.
19. Lee Y-B, Woo HY, Yoon C-B, Shim H-K. J Mater Chem 1999;9:2345.
20. Kuo EA, Hambleton PT, Kay DP, Evans PL, Matharu SS, Little E, McDowall N, Jones CB, Hedgecock CJ, Yea CM, Chan AW, Hairsine PW, Ager IR, Tully WR, Williamson RA, Westwood R. J Med Chem 1996;39:4608. [PubMed: 8917650]
21. Hanna PE, Gammans RE, Sehon RD, Lee MK. J Med Chem 1980;23:1038. [PubMed: 7411547]
22. Langenbeck VW, Rühlmann K, Reif HH, Stolze F. J Prakt Chem 1957;4:136.
23. *Compound* **4a**: yield 77%; mp 254–255 °C, lit. 264–266 °C;22 ^{1}H NMR (Varian Gemini 300, DMSO-d_6) δ 6.92 (d, 1H, *J* = 8.1 Hz), 7.21 (s, 1H), 7.25 (m, 2H), 7.35 (t, 2H, *J* = 7.2), 7.56 (d, 2H, *J* = 7.2 Hz), 7.75–7.81 (m, 2H), 11.12 (s, 1H); ^{13}C NMR (DMSO-d_6) δ 112.38, 118.22, 122.03, 126.34, 126.96, 127.51, 127.75, 128.61, 132.12, 136.16, 136.90, 149.69, 159.49, 184.35; EIMS (AutoSpec ETOF, Micromass) m/z 249 (M^+); HR-EIMS m/z calc. 249.078979, found 249.080332. *Compound* **4b**: yield 28%; mp 252 °C; ^{1}H NMR (DMSO-d_6) δ 6.94 (d, 1H, *J* = 8.1 Hz), 7.22 (1H, d, *J* = 16.5 Hz), 7.28–7.34 (m, 3H), 7.39 (t, 1H, *J* = 7.9), 7.52 (d, 1H, *J* = 7.8 Hz), 7.65 (s, 1H), 7.77–7.78 (m, 1H), 7.80 (dd, 1H, *J* = 8.2, 1.7 Hz); ^{13}C NMR (DMSO-d_6) δ 113.63, 119.41, 123.46, 126.35, 127.05, 127.46, 128.69, 130.03, 131.77, 132.87, 134.88, 137.78, 140.91, 151.28, 161.18, 185.92; EIMS m/z 283 (M^+); HR-EIMS m/z calc. 283.04001, found 283.03829. *Compound* **4c**: yield 5%; mp 230–235 °C; ^{1}H NMR (DMSO-d_6) δ 6.94 (d, 1H, *J* = 8.1 Hz), 7.06–7.09 (m, 2H), 7.24 (d, 1H, *J* = 16.5), 7.31 (d, 1H, *J* = 16.5 Hz), 7.39–7.43 (m, 3H), 7.77 (m, 1H), 7.80 (dd, 1H, *J* = 8.2, 1.7 Hz); ^{13}C NMR (DMSO-d_6) δ 113.55 (d), 115.35 (d), 119.55, 123.44, 124.06, 127.79, 129.91, 131.85 (d), 133.05, 137.75, 141.07 (d), 151.39, 161.04, 163.28, 164.90, 185.99; EIMS m/z 267 (M^+); HR-EIMS m/z calc. 267.069557, found 267.069991. *Compoud* **5**: yield 66%; mp 257–258 °C, lit. 261–265 °C. 22 ^{1}H NMR (DMSO-d_6) δ 7.09 (s, 1H), 7.29–7.43 (m, 6H), 7.50 (d, 1H, *J* = 7.8 Hz), 7.67 (dd, 2H, *J* = 7.1, 1.5 Hz), 11.10 (s, 1H); ^{13}C NMR (DMSO-d_6) δ 109.34, 116.77, 121.03, 125.14, 127.15, 127.61, 128.66, 128.74, 133.05, 136.22, 147.05, 151.19, 159.95, 183.20; EIMS m/z 249 (M^+); HR-EIMS m/z calc. 249.078979, found 249.079214.
24. Salach JI, Weyler W. Meth Enzymol 1987;142:627. [PubMed: 3600385]
25. Newton-Vinson P, Hubálek F, Edmondson DE. Protein Expr Purif 2000;20:334. [PubMed: 11049757]
26. Li M, Hubálek F, Newton-Vinson P, Edmondson DE. Protein Expr Purif 2002;24:152. [PubMed: 11812236]
27. Recombinant human liver MAO-A and MAO-B were expressed in *Pichia pastoris* and purified as described previously.25,26 The human MAO-B I199A mutant protein was constructed via site-directed mutagenesis. A manuscript is in preparation detailing the construction, expression, and purification protocol for the human MAO-B I199A mutant protein.
28. MAO activity measurements were performed spectrally using, as substrates, *p*-CF_3-benzylamine (MAO-A and MAO-B I199A mutant) and benzylamine (MAO-B) and following the formation of

their respective aldehyde products at 243 and 250 nm, respectively.29 Incubations were carried out at 25 °C in a 50 mM phosphate buffer (pH 7.5) containing 0.5% (w/v) reduced Triton X-100. K_i values were determined by measuring the initial rates of substrate oxidation at six different concentrations (50–3000 μM) in the absence and presence of three different inhibitor concentrations. All samples were incubated for 5 minutes at 25 °C prior to the addition of enzyme. K_i values were calculated by plotting the apparent K_m value recorded for each inhibitor concentration as a function of inhibitor concentration.

29. Walker MC, Edmondson DE. Biochemistry 1994;33:7088. [PubMed: 8003474]

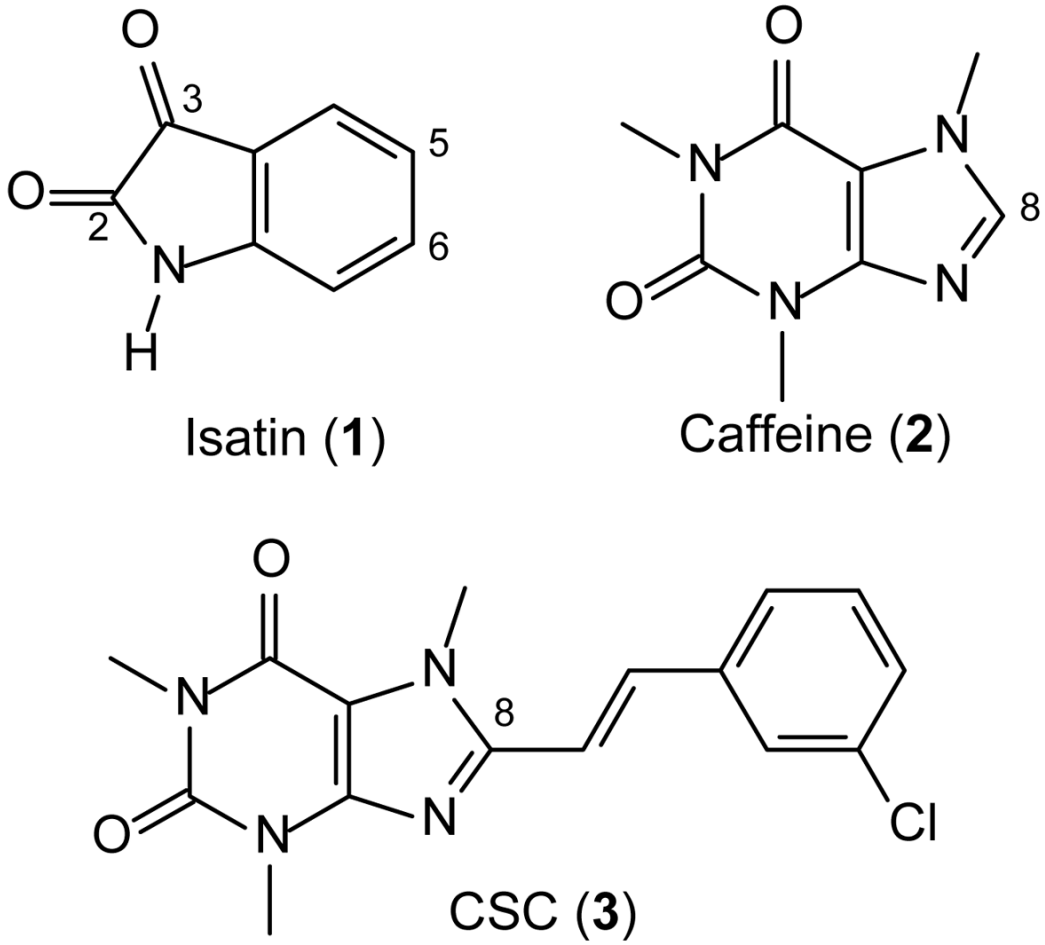

Figure 1.
The structures of isatin (**1**), caffeine (**2**) and CSC (**3**).

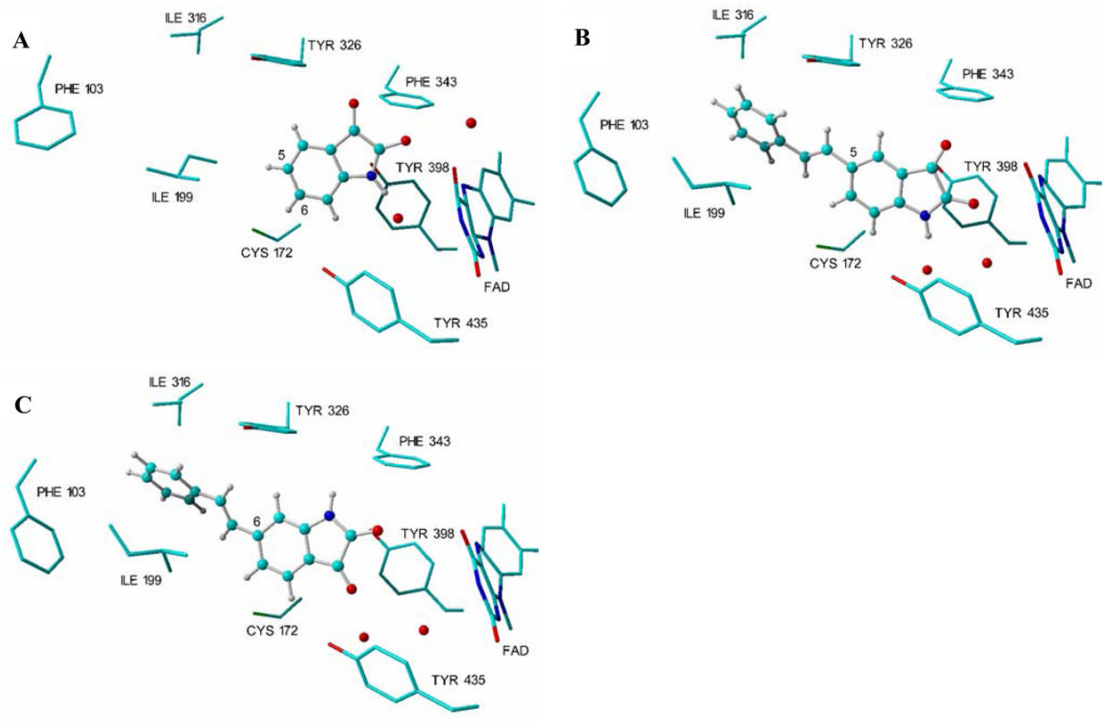

Figure 2.

The binding modes of isatin, **4a** and **5** in the active site of MAO-B. The three-dimensional structure of isatin in complex with human recombinant MAO-B (1OJA.pdb) is displayed in panel A[10] while the docking solutions of **4a** and **5** obtained with LigandFit are displayed in panel B and C, respectively. The models were generated in Yasara.[18]

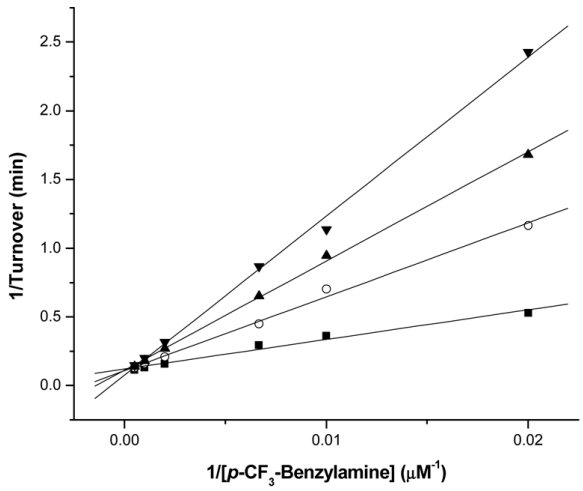

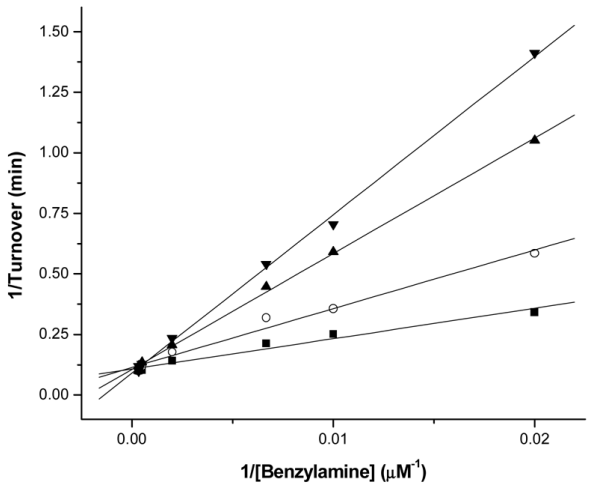

Figure 3.

Lineweaver–Burk plots of the recombinant human MAO-A (left) and MAO-B (right). The activity of MAO-A (Left) was assayed at varied concentrations of *p*-CF_3-benzylamine with constant inhibitor concentrations of: (■) 0.0 M of **4a**, (○) 1.0 M of **4a**, (▲) 2.0 M of **4a**, (▼) 3.0 M of **4a**.The activity of MAO-B (right) was assayed at varied concentrations of benzylamine with constant inhibitor concentrations of: (■) 0.0 M of **4a**, (○) 0.3 M of **4a**, (▲) 0.7 M of **4a**, (▼) 1.0 M of **4a**.

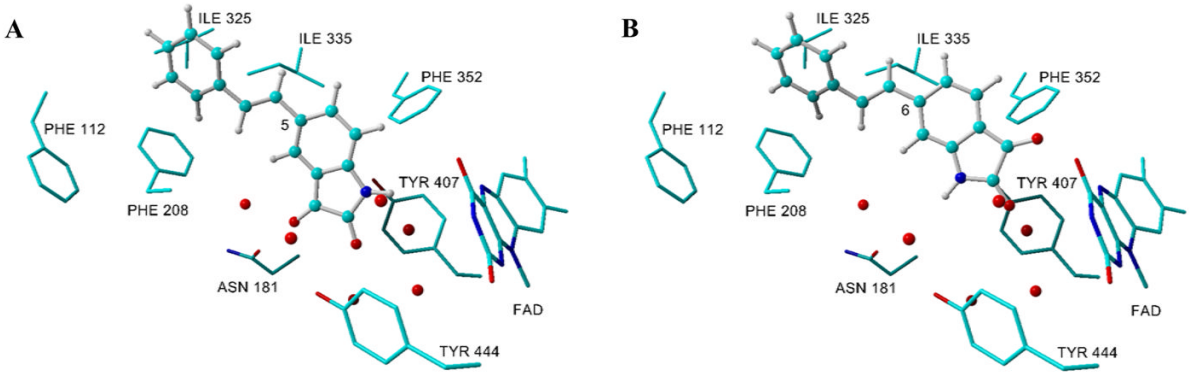

Figure 4.

The docking solutions obtained with LigandFit for the binding of **4a** (A) and **5** (B) in the active site of MAO-A (2Z5X.pdb).[14] The models were generated in Yasara.[18]

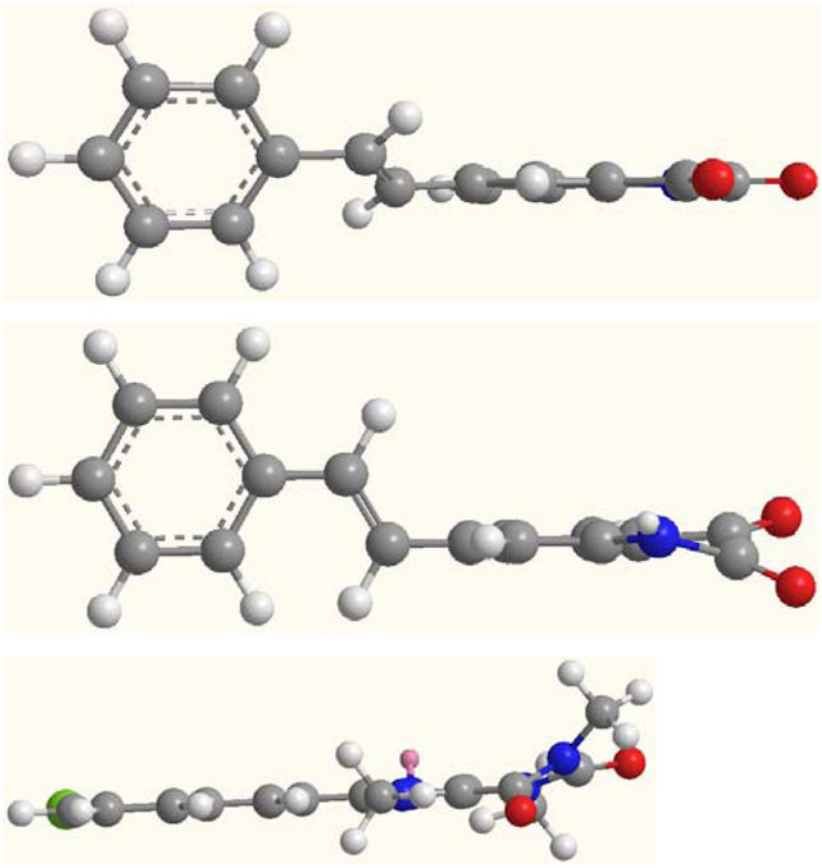

Figure 5.
Energy-minimized structures of **4a** (top), **5** (middle) and CSC (bottom). These structures and their energy-minimized conformations were constructed using Chem-3D (CambridgeSoft). The relative conformations of all structures are pictured with the isatin or caffeine rings being perpendicular to the plane of the page. Oxygen atoms are in red, nitogen atoms in blue and chlorine atoms in green.

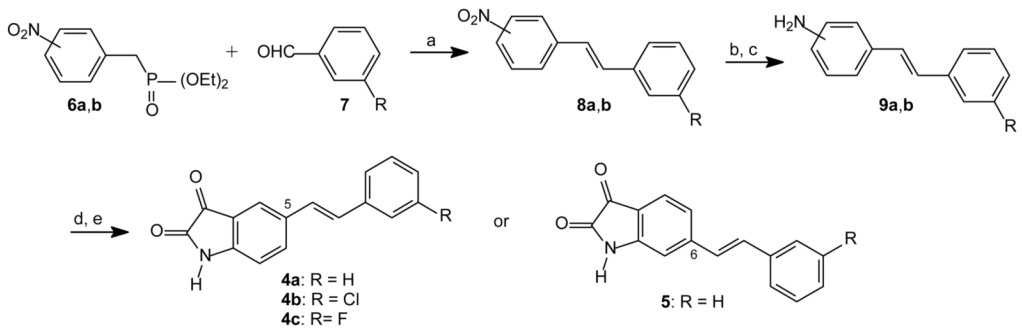

Scheme 1.

Synthetic pathway to analogues **4a**–**c** of (*E*)-5-styrylisatin and (*E*)-6-styrylisatin (**5**). Reagents and conditions: (a) NaOEt (b) $SnCl_2$/HCl, reflux (c) NaOH (d) diethyl ketomalonate, CH_3CO_2H, 120 °C (e) air, 120 °C.

Table 1

The IC_{50} values for the inhibition of baboon liver mitochondrial MAO-B by isatin (**1**) and (*E*)-styrylisatin analogues (**4**–**5**)

		IC_{50} value[a] (nM)
1	Isatin	8566 ± 530
4a	(*E*)-5-Styrylisatin	41.7 ± 1.8
4b	(*E*)-5-(3-Chlorostyryl)isatin	20.7 ± 0.6
4c	(*E*)-5-(3-Fluorostyryl)isatin	30.1 ± 4.6
5	(*E*)-6-Styrylisatin	444 ± 12.2

[a]The IC_{50} values were determined as described previously[12] and are expressed as the means ± SEM of duplicate determinations.

Table 2

The K_i values for the inhibition of purified recombinant human MAO by isatin (**1**) and (*E*)-styrylisatin analogues (**4**–**5**)

		MAO-A wild- type[a] (μM)	MAO-B wild-type[b] (μM)	MAO-B selectivity[c]	MAO-B I199A mutant[a] (μM)
1	Isatin	15[d]	3[d]	5.0	12 ± 2
4a	(*E*)-5-Styrylisatin	0.78 ± 0.10	0.31 ± 0.06	2.5	1.1 ± 0.2
4b	(*E*)-5-(3-Chlorostyryl)isatin	5.6 ± 0.3	1.4 ± 0.4	4.0	12.5 ± 0.7
4c	(*E*)-5-(3-Fluorostyryl)isatin	2.2 ± 0.2	0.60 ± 0.07	3.6	4.5 ± 0.2
5	(*E*)-6-Styrylisatin	22 ± 2	0.56 ± 0.02	39	2.2 ± 0.4

[a] The K_i values were determined spectrophotometrically using *p*-CF_3-benzylamine as substrate.

[b] The K_i values were determined spectrophotometrically using benzylamine as substrate.

[c] Selectivity for the B isoform is given as the ratio of K_i(MAO-A) to K_i(MAO-B) of the wild-type enzymes.

[d] Values obtained from reference.[9]